Refractive index and degree of inhomogeneity of nanocrystalline TiO_2 thin films: Effects of substrate and annealing temperature

Md. Mosaddeq-ur-Rahman
Venture Business Laboratory, Nagoya Institute of Technology, Gokiso-cho, Showa-ku, Nagoya 466-0856, Japan

Guolin Yu
Research Center for Micro-Structure Devices, Nagoya Institute of Technology, Gokiso-cho, Showa-ku, Nagoya 466-0856, Japan

Tetsuo Soga and Takashi Jimbo
Department of Environmental Technology and Urban Planning, Nagoya Institute of Technology, Gokiso-cho, Showa-ku, Nagoya 466-0856, Japan

Hiroshi Ebisu and Masayoshi Umeno
Department of Electrical and Computer Engineering, Nagoya Institute of Technology, Gokiso-cho, Showa-ku, Nagoya 466-0856, Japan

(Received 29 December 1999; accepted for publication 5 July 2000)

Nanocrystalline TiO_2 thin films, deposited on single crystal Si (100) substrates under different temperature conditions by the sol–gel dip coating method, have been investigated for their optical properties using ultraviolet-visible spectroscopic ellipsometry. A gradual increase in refractive index, *n*, with increasing annealing temperature up to 600 °C, and thereafter a sharp increase in *n* at 800 °C of annealing temperature have been observed. For the heat-treated and low temperature (400 °C) annealed films, *n* is found to be higher at the film–substrate interface than at the film surface and the refractive index gradient slightly increases for the annealed sample. However, for the 600 °C temperature annealed film, the refractive index gradient significantly decreases and the film appears to be almost homogeneous. These results are in sharp contrast with those for the films deposited on a vitreous silica substrate where *n* was found to be higher at the film surface than at the film–substrate interface and the refractive index gradient increased with increasing annealing temperature. For the high temperature (800 °C) annealed sample on the Si substrate, formation of a thick SiO_2 interfacial layer has been observed and the degree of homogeneity deteriorates severely.
 [S0021-8979(00)00820-3]

I. INTRODUCTION

Titanium dioxide is a large band gap semiconductor of exceptional stability that has diverse industrial applications. TiO_2 thin films with their high refractive index have broad applications in optical coatings and waveguides.[1–6] In recent years, sol–gel derived nanocrystalline TiO_2 thin films of anatase phase have become of increasing importance because of their ease of preparation and potential application in the areas of photovoltaics, sensing devices, photocatalysis, and microelectronics.[7] Consequently, determination of the optical constants and evaluation of microstructural features such as surface roughness in these films are important.

Wide variations in the optical and physical properties of TiO_2 thin films deposited by different techniques have been reported.[8] For sol–gel derived films, film properties such as crystallinity, particle size, degree of homogeneity, etc. depend largely on annealing temperature and substrate topography. The aim of this work is to study the effects of substrate and annealing temperature on the optical constants and degree of inhomogeneity of sol–gel derived TiO_2 thin films. Spectroscopic ellipsometry (SE), which is known to be a very useful and nondestructive technique with which to investigate the optical properties of inhomogeneous films, has been used to study our films. Ellipsometric determination of optical constants of inhomogeneous TiO_2 films deposited by different evaporation techniques has been reported by various authors where they assumed a linear variation in the refractive index along the thickness of the film.[9,10] In a previous communication, we described a model for the determination of optical constants of sol–gel derived TiO_2 thin films by spectroscopic ellipsometry where void distribution was assumed instead of the variation in the refractive index (*n*) along the thickness of the film and the unknown dielectric function of TiO_2 was described by a single oscillator form.[11] In that model, a four-layer structure (air/rough surface layer/inhomogeneous TiO_2 layer/substrate) was used to fit the SE data. In this article, we study TiO_2 films deposited on a Si substrate using the same model, however, an additional interfacial layer between the TiO_2 film and substrate has been assumed for the higher temperature annealed films in order to obtain a good fit. Excellent agreement between the calculated and measured data of SE in the 335–830 nm wavelength range has been obtained. Details of experimental procedures and results and discussion are given in the following.

TABLE I. Experimental conditions of sol–gel derived TiO_2 thin films.

Sample No.	Drying	Heat treatment	Annealing
1	80 °C for 15 min	400 °C for 1 h	···
2	80 °C for 15 min	400 °C for 1 h	400 °C for 6 h
3	80 °C for 15 min	400 °C for 1 h	600 °C for 6 h
4	80 °C for 15 min	400 °C for 1 h	800 °C for 6 h

II. EXPERIMENT

TiO_2 thin films were deposited on a single crystal Si (100) substrate by the sol–gel method using titanium tetraisopropoxide, $Ti(C_3H_7O)_4$, as the starting material for Ti. Details of the sol solution preparation are described elsewhere.[12]

Films were coated onto the substrate by the dip-coating method with a pulling speed of 0.1 mm/s. Prior to deposition, the substrates were cleaned with acetone and methanol successively using an ultrasonic cleaner, etched with 10% HF aqueous solution for 1 min, rinsed with distilled water, and then, blown dry with N_2. The films thus coated were dried at 80 °C for 15 min and heat treated at 400 °C for 1 h. The process was repeated five times and finally the films were annealed at 400, 600, and 800 °C, respectively, for 6 h in air. For annealing, the temperature was first raised to the desired temperature at a constant heating rate of 5 °C/min, kept at that temperature for 6 h, and then cooled down at the same rate. However, at around 300 °C, the rate of cooling fell below 5 °C/min, and the two ends of the tubular furnace were opened to allow fast cooling. The drying heat treatment, and annealing conditions for all the samples are summarized in Table I.

The crystal structure, growth, and crystallinity of various phases of these films were studied by x-ray diffraction (XRD) (Rigaku Rint-1100) using Cu $K\alpha$ radiation (1.5406 Å) as an x-ray source. All the patterns were recorded at a scanning rate of 1° min^{-1} in steps of 0.4° in standard θ–2θ geometry with 40 kV voltage and 30 mA current for x-ray excitation. Cross-sectional views of the films were observed by a high-resolution scanning electron microscope (Hitachi S-5000). Formation of a silicon oxide layer usually takes place at the interface when metal oxides are deposited on the Si substrate using the sol–gel technique at high annealing temperature.[13] The nature of any such interfacial layer, if present, at the Si and TiO_2 interfaces was characterized by Fourier transform infrared (FTIR) spectroscopy.

Measurements of spectroscopic ellipsometry were carried out at an angle of incidence of 70° in the wavelength range of 335–830 nm. The automatic ellipsometry used was of rotating analyzer type, fitted with a 75 W xenon lamp as a light source. The optical properties of the thin films were fitted directly to measured SE (Δ, Ψ) data using a classical dispersion formula. All the measurements were performed at room temperature. Although details of the theoretical treatment for ellipsometric measurement of an inhomogeneous film have been discussed in our earlier publication,[11] a brief overview will be given here.

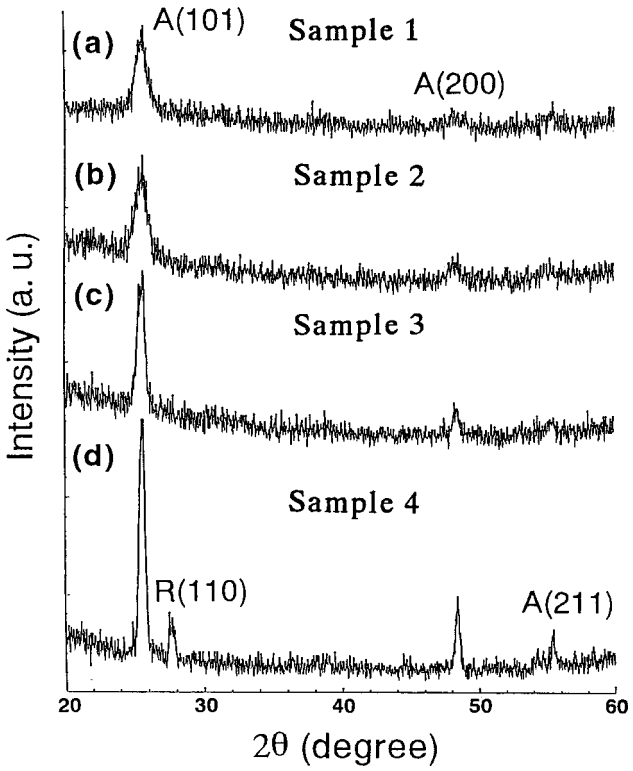

FIG. 1. X-ray diffraction patterns of heat-treated and annealed nanocrystalline TiO_2 thin films, deposited on a Si substrate (A: anatase, R: rutile).

The ellipsometric parameters Ψ and Δ are defined as usual from the ratio of reflected amplitudes for *s* and *p* polarization,

$$\rho = \frac{r_P}{r_s} = \frac{|r_P|}{|r_s|} e^{i(\delta_P - \delta_s)} = \tan\Psi e^{i\Delta}. \tag{1}$$

In the case of an inhomogeneous film, the refractive index of the film is not uniform but varies as a function of distance along the thickness of the film. Under the simplifying assumption that the reflection of light from the interior of the film can be ignored, detailed expressions of Ψ and Δ have been given by Carniglia.[14] It has also been shown by Carniglia that ellipsometric data at half-wave (HW) points, defined as wavelengths that are multiples of twice the optical thickness, in the $\tan\Psi$ spectrum [hereafter referred to as $\tan\Psi$ (HW)], offers a sensitive measure of the degree of inhomogeneity. In particular, when the film is homogeneous, $\tan\Psi(\mathrm{HW}) = \tan\Psi_s$, where $\tan\Psi_s$ is amplitude reflectance ratio of the uncoated substrate, showing that for homogeneous film $\tan\Psi(\mathrm{HW})$ is independent of the index of the film. Thus, from the difference between $\tan\Psi_s$ and $\tan\Psi(\mathrm{HW})$, one can get an idea about the degree of inhomogeneity of a film which is defined by $\Delta n/\bar{n}$; here $\bar{n}$ is the average refractive index of the film and $\Delta n = n_1 - n_2$, where n_1 and n_2 are the refractive indices at the outer and inner surfaces of the film, respectively.

The Bruggeman effective-medium theory (EMT), considered an important tool to investigate inhomogeneous film, is used to calculate the effective dielectric function of the film. The mathematical formula can be expressed as[15]

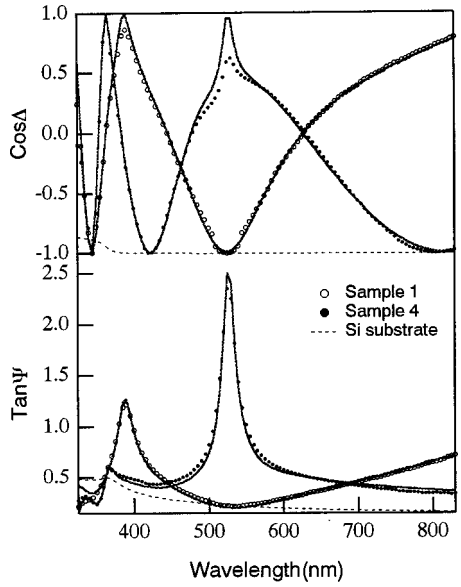

FIG. 2. Measured (closed and open circles) and fitted (solid lines) cos Δ (top) and tan Ψ (bottom) spectra of samples 1 and 4, together with the calculated data of a bare substrate (dashed lines).

$$(1-f_v)\frac{\varepsilon_m-\varepsilon}{\varepsilon_m+2\varepsilon}+f_v\frac{1-\varepsilon}{1+2\varepsilon}=0, \tag{2}$$

where ε_m is the dielectric function of the main constituent material and f_v is the volume fraction of void. In this equation the dielectric function of void is taken to be 1. In our SE data analysis, the unknown dielectric function of TiO_2 is described by a single oscillator,[16]

$$\varepsilon=n^2-k^2+2ink=\varepsilon'_\infty+\frac{(\varepsilon_s-\varepsilon'_\infty)\omega_t^2}{\omega_t^2-\omega^2+i\Gamma_0\omega}, \tag{3}$$

where ε'_∞ represents the high-frequency dielectric constant, ε_s the static dielectric constant, ω_1 the frequency, and Γ_0 the damping factor of the oscillator. The unknown parameters can be numerically determined by minimizing the following mean squares deviation with a regression program (unbiased):

$$\delta^2=\frac{1}{2N-P}\sum_i^N[(\tan\Psi_i^{\exp}-\tan\Psi_i^{\text{cal}})^2+(\cos\Delta_i^{\exp}-\cos\Delta_i^{\text{cal}})^2], \tag{4}$$

where N is the number of data points and P is the number of unknown model parameters.

III. RESULTS AND DISCUSSION

A. X-ray diffraction

XRD patterns of TiO_2 thin films, both heat treated and annealed at different temperature conditions, deposited on the Si substrate, are shown in Fig. 1. All the peaks are indexed according to standard JCPDS patterns for the TiO_2 lattice.[17] As is evident from these patterns, the films are polycrystalline, single phase, anatase (A) type, except for the sample annealed at 800 °C where presence of an x-ray peak corresponding to the (110) plane of rutile (R) phase is also observed. These observations are in agreement with those reported by Yuan and Tsujikawa[18] for sol–gel derived TiO_2 powder where they found it to be anatase type up to 600 °C annealing temperatures and above that (600–900 °C) a mixture of anatase/rutile. Although the anatase/rutile transformation temperature is around 600–700 °C, our films are predominantly of anatase type even at 800 °C with crystals oriented preferentially in the (101) plane as can be seen from the intense x-ray peak corresponding to the A(101) plane of anatase modification of the TiO_2 lattice. The x-ray patterns also show a gradual decrease in the full width at half maximum (FWHM) of the x-ray peak corresponding to the

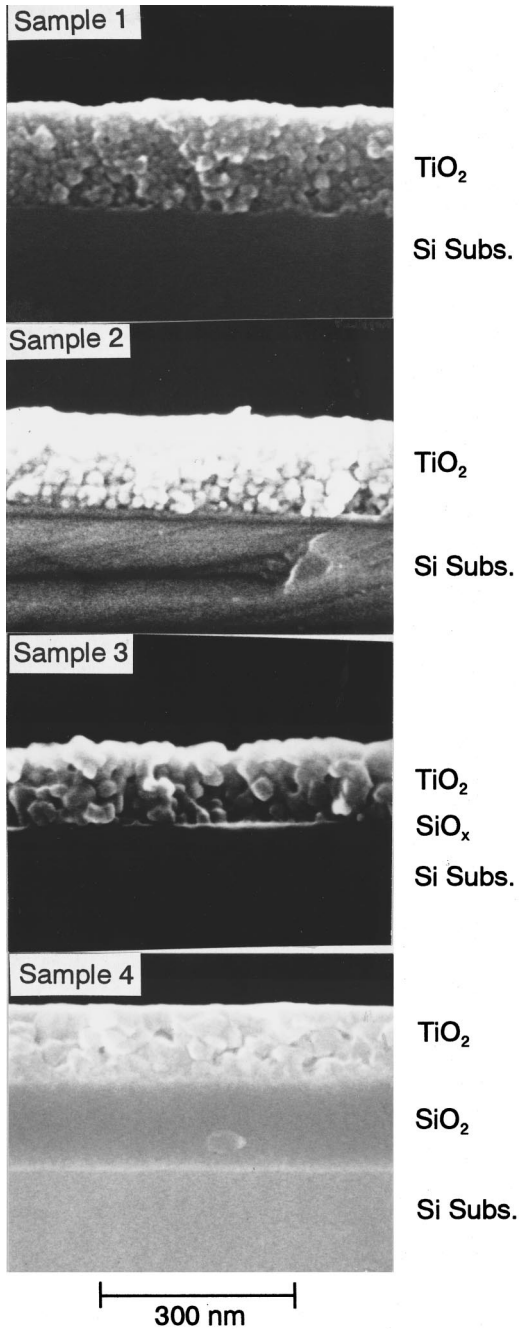

FIG. 3. Cross-sectional scanning electron micrographs of heat-treated and different temperature annealed nanocrystalline TiO_2 thin films, deposited on a Si substrate.

TABLE II. Lists of coefficients of the classical dispersion formula, void fraction at the inner surface of the TiO_2 film (f_{vi}) void fraction of the interfacial layer (f_i), and thicknesses of the rough layer (d_1), TiO_2 film (d_2), and the interfacial layer (d_3) for all the samples, obtained by fitting of SE data. The 90% confidence limit are given by ($\pm$).

Sample No.	$\varepsilon'_\infty(n^2_\infty)$	$\varepsilon(n^2_s)$	ω_t (eV)	Γ_0 (eV)	f_{vi}	f_i	d_1 (nm)	d_2 (nm)	d_3 (nm)	δ
1	2.62 ± 0.01	3.49 ± 0.01	4.25 ± 0.01	0.095 ± 0.002	-0.085 ± 0.002		1.62 ± 0.1	145.3 ± 0.2		0.026
2	2.59 ± 0.02	3.58 ± 0.03	4.28 ± 0.02	0.114 ± 0.004	-0.093 ± 0.005		1.8 ± 0.2	144.4 ± 0.2		0.040
3	2.53 ± 0.07	3.95 ± 0.07	4.22 ± 0.03	0.20 ± 0.01	0.005 ± 0.02	0.33 ± 0.03	0 ± 0.3	114.8 ± 3	19.4 ± 2	0.044
4	5.12 ± 0.01	5.93 ± 0.01	4.04 ± 0.01	0.197 ± 0.002	0.327 ± 0.009	0.640 ± 0.005	5.4 ± 0.1	119.0 ± 0.3	142.2 ± 1	0.062

A(101) plane with increasing annealing temperature, indicating improved crystallinity. The crystallite sizes deduced from the linewidths of the A(101) plane using the Scherrer equation[19] are found to be approximately 7.4, 8.5, 15.3, and 23.4 nm for the heat-treated and 400, 600, and 800 °C annealed samples, respectively. The crystallite sizes of the four samples observed by scanning electron microscope (SEM) surface morphology are 7–9, 8–10, 15–25, and 25–75 nm, respectively. The particle sizes determined from x-ray linewidths match closely the minimum particle sizes observed by SEM. Since the sharper x-ray linewidths of the bigger particles get buried in the broader linewidths coming from the smaller particles, it is only possible to determine the minimum size of the crystallites present in the film from the x-ray linewidths.

In order to determine the crystallographic preferred orientation of growth, we have calculated the normalized intensity ratio β of each sample defined as $\beta = I_{i(200)}/I_{P(200)}$, where $I_{i(200)} = C_{i(200)}/C_{i(101)}$ is the intensity ratio of the Bragg peaks of the diffraction profiles recorded and $I_{P(200)}$ is the intensity ratio of the Bragg peaks for the standard randomly oriented TiO_2 powder which is 0.35 as obtained from JCPDS powder diffraction file No. 21-1272 for anatase TiO_2 powder. The β values obtained for samples 1–4 are 0.44 ± 0.09, 0.51 ± 0.10, 0.62 ± 0.03, and 0.83 ± 0.008, respectively. The $\pm$ term shows the uncertainty with which (200) peak intensity has been measured. This result indicates highly preferred orientation of the A(101) plane for sample 1 which gradually diminishes with annealing time and temperature. Similar preferred orientation has also been observed for films deposited on quartz and sapphire substrates. Preferred orientation of the A(101) plane was also reported by Kato *et al.*[20] for sol–gel derived TiO_2 films deposited on a quartz substrate by the dip-coating method using a titanium tetraisopropoxide-ethanol-diethanolamine-water solution. No amorphous background is observed in any of the patterns. This is also in agreement with the observation made by Yuan and Tsujikawa that an amorphous to crystalline transition occurs in the temperature range of 300–400 °C for sol–gel derived TiO_2.

B. Spectroscopic ellipsometry

A five-phase structure (air/rough surface layer/inhomogeneous TiO_2/interfacial layer/substrate) has been used in the simultaneous fitting of measured parameters Δ and Ψ of SE. The rough layer on the surface was modeled as an effective mixture of 50% TiO_2 and 50% void. Inhomogeneity of a film results from the nonuniform packing density of the film which is usually expressed by the volume fraction of void f_v. In our fitting analysis f_v is varied from $f_{vo}=0$ at the outer surface of the film to f_{vi} at the inner surface. f_v obtained by such a fitting analysis shows only a relative variation in the void fraction along the thickness of the film and the change in refractive index along the depth of the film will follow the change in f_v. After obtaining the refractive index by fitting to SE data, actual void distribution along the depth of the film has been calculated using the ''void-free'' refractive index of TiO_2.[21] The refractive index of a dense anatase film considered void free has been taken from Ref. 21 and is used to calculate the actual void distribution using the expression $(n_{vf}-n_f)/n_{vf}$, where n_{vf} is the refractive index of the void-free dense anatase film and n_f is the refractive index obtained by fitting analyses. For the heat-treated and low temperature annealed films, a very good fit has been obtained without considering any interfacial layer. However, it is found that for higher temperature (600 and 800 °C) annealed samples an interfacial layer has to be considered to get a reasonably good fit. The interfacial layer is characterized for optical properties by the same dispersion formula as that of TiO_2 except that a different void fraction f_i of the constant value along the thickness has been assumed.

Measured (open and closed circles) and fitted (solid lines) $\cos\Delta$ (top) and $\tan\Psi$ (bottom) spectra of samples 1 and 4, together with the calculated data of a bare substrate (dashed lines), are shown in Fig. 2. Excellent agreement between the experimental and fitted $\cos\Delta$ and $\tan\Psi$ spectra for both the samples has been obtained. From Fig. 2, it can be clearly seen that at HW fringes $\tan\Psi(\mathrm{HW}) \neq \tan\Psi$, for both the samples, indicating inhomogeneity in the films. Further, although for sample 1 $\tan\Psi(\mathrm{HW})$ is very close to $\tan\Psi_s$, it is separated by a big distance from $\tan\Psi_s$ for sample 4, showing very high inhomogeneity for this sample, which is annealed at a very high temperature (800 °C).

Table II shows the best fit model parameters used in the simulation of $\cos\Delta$ and $\tan\Psi$ spectra. A decrease in the thickness with increasing annealing temperature is observed, due to increased packing density of the films as evidenced by SEM cross-sectional micrographs (Fig. 3), which show a nanocrystalline porous structure of the films with increasing particle size and decreasing void with annealing temperature. Similar results were also reported by Vorotilov *et al.*[22] for sol–gel derived TiO_2 thin films. While the unannealed and low temperature annealed samples show no detectable inter-

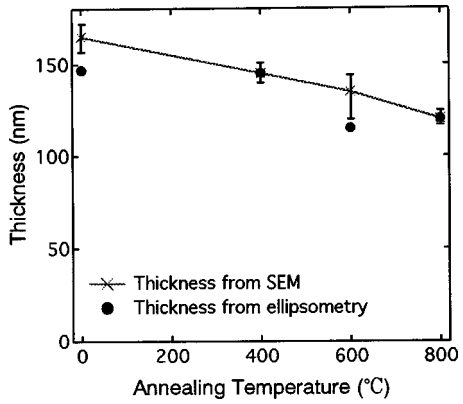

FIG. 4. Plot of TiO_2 layer thickness vs annealing temperature for heat-treated and annealed TiO_2 thin films.

facial layer by SEM, an interfacial layer (~140 nm, by SEM) thicker than that of TiO_2 film (~120 nm, by SEM) is observed for the high temperature annealed sample. The film thicknesses obtained for both the TiO_2 and the interfacial layers by spectroscopic ellipsometry are in good agreement with the SEM cross-sectional thickness measurements. Figure 4 shows a pictorial representation of the gradual decrease in film thickness with increasing annealing temperature.

Figure 5 shows the refractive index spectrum of the interfacial layers for samples 3 and 4 together with that for pure SiO_2. Although the refractive indices of the interfacial layer of sample 3 are very different from these of pure SiO_2 (Fig. 5, dotted line), the refractive indices for that of sample 4 match very well with those of pure SiO_2 at longer wavelengths. At shorter wavelengths, due to absorption by the top TiO_2 layer, it is not possible to extract the correct values of refractive indices of the interfacial layer by the fitting analysis of SE data. These results are further crosschecked by examining the nature of the interfacial layers using Fourier transform infrared spectroscopy. Figure 6 shows the IR transmission spectra of all the samples. The three absorption bands at 1080, 810, and 459 cm^{-1} for sample 4 are characteristic IR features of SiO_2 and correspond to stretching, bending, and rocking vibrations of the Si–O–Si bond, respectively. The sharp absorption band at 1080 cm^{-1} together with the broad shoulder at the higher frequency side shows the presence of stoichiometric SiO_2 for the 800 °C temperature annealed sample.[23] However, for sample 3, where the absorption is very weak due to much lower thickness of the interfacial layer, the absorption band is slightly shifted towards the lower frequency side (1069 cm^{-1}), indicating that the interfacial layer is not purely stoichiometric SiO_2. No clear absorption peaks in the IR spectra are observed for the unannealed and low temperature annealed films which show the absence of any detectable interfacial oxide layer and conform with the results of SE analyses and SEM micrographs.

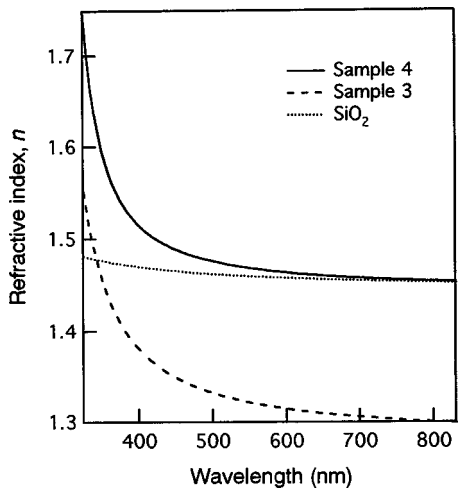

FIG. 5. Plot of refractive indices of the interfacial layers of 600 and 800 °C temperature annealed samples together with that of pure SiO_2.

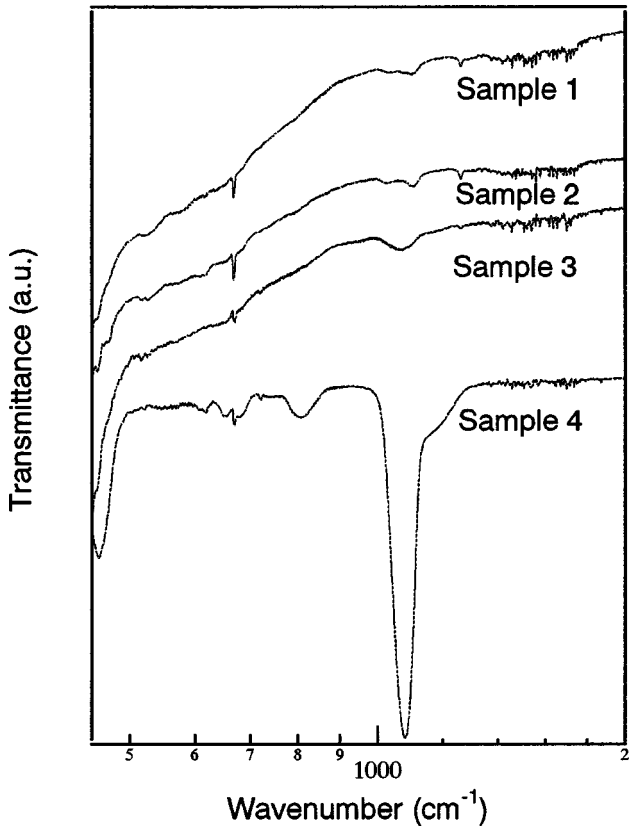

FIG. 6. FTIR spectra of heat-treated and annealed nanocrystalline TiO_2 thin films, deposited on a Si substrate.

As shown in Table II, f_{vi}, the void fraction at the inner surface of the TiO_2 film is negative for samples 1 and 2, indicating that the films are more dense at the interface than at the outer surface since the void fraction at the surface is considered to be zero. Although for both samples 3 and 4, f_{vi} is positive, it is very small and close to zero for sample 3, showing almost uniform void distribution, but very high for sample 4, indicating high nonuniformity of this sample.

As shown in Table II, the high frequency dielectric constants obtained by fitting analyses of SE data are 2.62, 2.59, 2.53, and 5.12 for samples 1, 2, 3, and 4, respectively. However, as pointed out by Gerfin and Gratzel for ITO films,[16] here also ε'_∞ does not represent the true high-frequency dielectric constant ε_∞. The optimized dispersion formula can be regarded only as a mathematical description of the optical

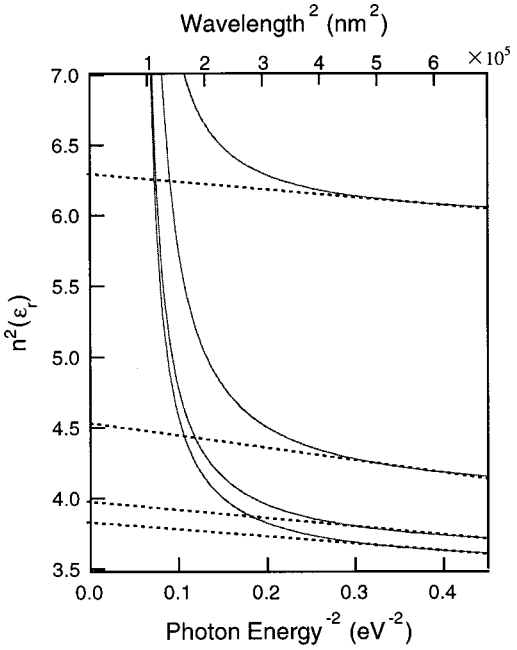

FIG. 7. Graphical determination of the high-frequency dielectric constant of all the samples.

properties below the band edge region of the semiconductor. The value of ε_∞ can be determined graphically, as shown in Fig. 7 and are found to be 3.82, 3.96, 4.5, and 6.27 for samples 1, 2, 3, and 4, respectively. The corresponding values of refractive indices at high frequency, n_∞, are 1.95, 1.99, 2.12, and 2.5, respectively, for the four samples. Although for samples 1, 2, and 3 the values of the high frequency dielectric constants are close to that determined by Kim for a void-free value (4.8) of electron-beam-evaporated TiO_2 thin film,[21] from sample 4, which is annealed at a much higher temperature, it is quite high, and may be due to the larger crystallite size, higher packing density, and presence of the rutile phase along with the anatase, which has higher refractive indices.

In Fig. 8, we show the refractive index n (top) and extinction coefficient k (bottom) spectra at the surface of the samples over the wavelength range of 335–800 nm. There is a gradual increase in n as the as-deposited samples are annealed at higher temperatures (up to 600 °C) and at a much more elevated temperature (800 °C), a sharp increase in n is observed (Fig. 8, top). This increase in n with annealing temperature is attributed to the increase in packing density and crystallinity of the films which are also evident from the thickness measurement and XRD analysis. Furthermore, the sharp increase in n above 600 °C may be due to the enhanced crystallinity of the TiO_2 films and formation of the rutile phase along with the anatase at this elevated temperature, evidenced by the x-ray analysis (XRD pattern 4, Fig. 1).

Measurement of k, where absorption is very small, is not very accurate with spectroscopic ellipsometry. However, within the accuracy limit, the k spectra do not show any significant absorption in the wavelength region lower than the band gap energy of the anatase form of TiO_2 3.2 eV. The sharper increase in k above the fundamental band gap for

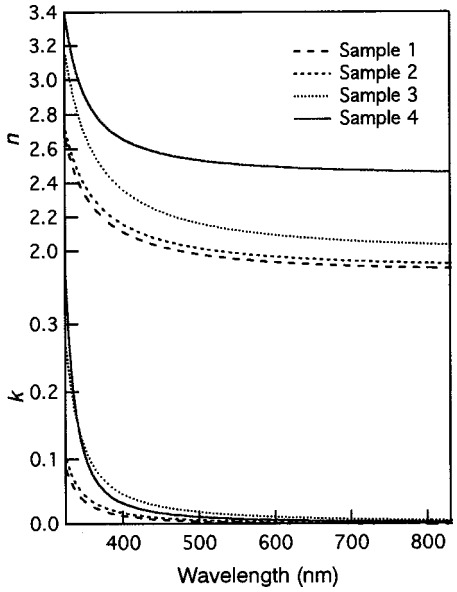

FIG. 8. Refractive index n (top) and extinction coefficient k (bottom) spectra at the surface of nanocrystalline TiO_2 thin films, deposited on Si substrates.

samples 3 and 4 is probably due to higher crystallinity for the high temperature annealed samples. Note that the nonzero extinction coefficient for all the samples at a lower photon energy than the band gap energy indicates a scattering effect in the nanocrystalline TiO_2 thin film which increases for high temperature annealed samples due to larger particle size. The presence of voids in the film may also lead to a nonzero extinction coefficient.

In Fig. 9, we show the grading profiles of the refractive index for all the samples at 500 nm wavelength along with those for the films deposited on the vitreous silica substrate, lines q400 and q600 for the 400 and 600 °C temperature annealed films, respectively, reported in our previous communication[11] for comparison. An almost linear index gradient along the depth of the films has been obtained. For the heat-treated and low temperature annealed samples, the

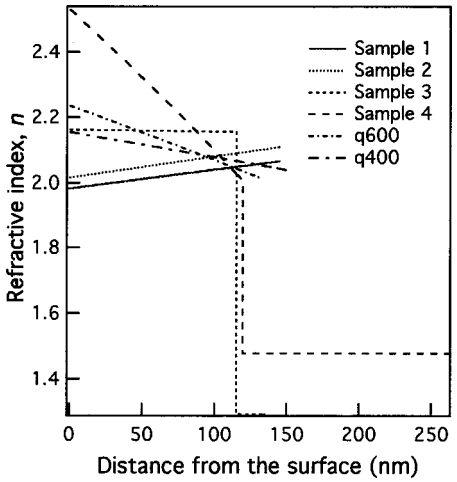

FIG. 9. Depth profiles of the refractive indices for all the samples at 500 nm wavelength. Lines q400 and q600 represent the depth profiles of the films deposited on a vitreous silica substrate, annealed at 400 and 600 °C, respectively, reported previously (see Ref. 5) which are included for comparison.

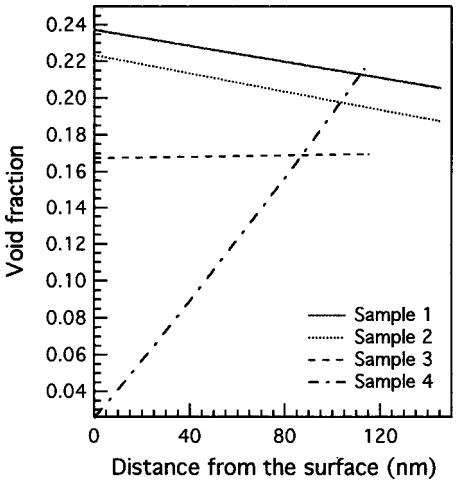

FIG. 10. Variation of void fraction along the thickness of the TiO_2 films.

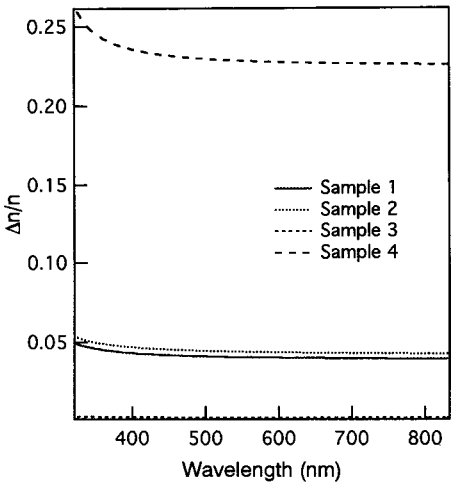

FIG. 11. Variation of the degree of inhomogeneity $\Delta n/\bar{n}$ with photon energy for all the samples.

refractive index is highest at the interface and gradually decreases towards the outer surface with the refractive index gradient slightly increasing for the annealed sample. This trend is completely opposite to that what is obtained for films deposited on the vitreous silica substrate annealed at 400 and 600 °C. This difference in grading profiles between the films deposited on two different substrates is probably due to the difference in substrate topography. Vitreous silica is an amorphous substrate which inhibits crystallization, therefore crystallization and densification begin at the surface of the deposited film which gradually progresses towards the interface during the course of annealing, thus giving higher refractive indices at the surface.[24] On the other hand, silicon is a crystalline substrate, therefore crystallization of the deposited films starts from the silicon surface and gradually progresses towards the film surface resulting in higher refractive indices at the interface than at the film surface. However, this situation holds for low annealing temperature conditions only. As the annealing temperature increases beyond 400 °C, an interfacial silicon oxide layer is formed which retards the crystallization process at the interface. At this point, the substrate behaves like an amorphous one, and crystallization and densification are more pronounced at the outer surface than at the interface. In the case where the annealing temperature is 600 °C, the two effects, first the crystallization at the interface at low annealing temperature and later that at the outer surface at high annealing temperature, seem to balance out, resulting in a quite homogeneous film as can be seen from Fig. 9 which shows an almost constant refractive index along the thickness for sample 3. However, for sample 4, which is annealed at 800 °C, the latter effect seems to outdo the former one, resulting in a very high refractive index at the surface. Furthermore, the refractive index at the interface for sample 4 is below that of sample 3, maybe due to diffusion of Si atoms into the TiO_2 layer at this high temperature.

Variation in the void fraction along the thickness of the films calculated using the void-free refractive index of a dense film taken from Ref. 21 is shown in Fig. 10. High void fraction can be seen for sample 1 which decreases with annealing time and temperature. An average void fraction of 0.16 has been reported for electron-beam evaporated TiO_2 thin film by Kim. For sol-gel derived films, all the films seem to have higher void fraction than the electron-beam evaporated film except the 800 °C annealed film which shows a very low void fraction near the film surface, indicating the dense nature of the film. Figure 11 shows the variation in the degree of inhomogeneity with wavelength for different samples. For all the samples variation in the degree of inhomogeneity with wavelength follows the same trend as that of the refractive index which gradually decreases with increasing wavelength. Whereas the low temperature annealed sample shows a slightly higher degree of inhomogeneity than the unannealed one, the higher temperature (600 °C) annealed sample shows a very small degree of inhomogeneity which is in sharp contrast with the results obtained for films deposited on the vitreous silica substrate where the degree of inhomogeneity greatly increased for the same annealing conditions, from 5%–6% to 12%–14%.[11] The degree of inhomogeneity of samples 1 and 2 (4.8%–5.1%) is very close to those reported for TiO_2 films deposited by electron-beam (EB) evaporation (3%–5%) and radio-frequency (rf) sputtering (5%) techniques.[8] However, for sample 4, annealed at a much higher temperature (800 °C), the degree of inhomogeneity is as high as 25%, indicating severe inhomogeneity in the film. Thus it is evident that very high temperature annealing severely deteriorates the degree of homogeneity of a film.

IV. CONCLUSIONS

A detailed optical characterization of sol–gel derived nanocrystalline TiO_2 thin films, deposited on single crystal Si (100) substrates under different temperature conditions, has been carried out by ultraviolet-visible spectroscopic ellipsometry. XRD patterns reveal a polycrystalline, single phase, anatase polymorph with preferred orientation of the $A(101)$ plane up to 600 °C annealing temperature and a mixture of anatase/rutile at 800 °C. SEM cross-sectional micrographs show the nanocrystalline porous structure of the films with increasing particle size, decreasing thickness, and a lesser void with increasing annealing temperature.

Optical properties, n and k, of the thin films were fitted directly to measured SE (Δ, Ψ) data using the classical dispersion formula. A gradual increase in the refractive index, n, with increasing annealing temperature up to 600 °C has been observed due to the increase in crystallization and densification as observed by XRD patterns and SEM micrographs. The sharp increase in n at a much elevated temperature (800 °C) may be due to enhanced crystallinity at this temperature along with the presence of the rutile phase as observed by the XRD patterns. Further, for the heat-treated and low temperature (400 °C) annealed films, n is found to be higher at the film–substrate interface than at the film surface and the refractive index gradient slightly increases for the annealed sample. However, for the 600 °C temperature annealed film, the refractive index gradient significantly decreases and the film appears to be almost homogeneous. These results are completely opposite to that what we obtained for films deposited on the vitreous silica substrate annealed at 400 and 600 °C, where n was found to be higher at the outer surface of the film than at the film–substrate interface, with the refractive index gradient increasing with annealing temperature. This difference in grading profiles for films deposited on the two different substrates is explained in terms of substrate topography. Formation of an interfacial silicon oxide layer has been observed for the films deposited on the Si substrate when annealed above 400 °C. For the 800 °C annealed sample, the degree of homogeneity has been found to deteriorate severely along with the formation of a very thick interfacial SiO_2 layer. This study shows that the degree of inhomogeneity depends strongly on the annealing temperature as well as on the substrate topography.

[1] J. C. C. Fan and F. J. Bachner, Appl. Opt. **15**, 1012 (1976).
[2] Y. Paz, Z. Luo, L. Rabenberg, and A. Heller, J. Mater. Res. **10**, 2842 (1995).
[3] J. Mugnier, B. Varrel, M. Bahtat, C. Bovier, and J. Serughetti, J. Mater. Sci. Lett. **11**, 875 (1992).
[4] A. Bahtat, M. Bouazaoui, M. Bahtat, and J. Mugnier, Opt. Commun. **111**, 55 (1994).
[5] A. Bahtat, M. Bouderbala, M. Bahtat, M. Bouazaoui, J. Mugnier, and M. Druetta, Thin Solid Films **323**, 59 (1998).
[6] T. W. Kim, M. Jung, H. J. Kim, T. H. Park, Y. S. Yoon, W. N. Kang, S. S. Yom, and H. K. Na, Appl. Phys. Lett. **64**, 1407 (1994).
[7] M. Gratzel, in *Semiconductor Nanoclusters—Physical, Chemical and Catalytic Aspects*, edited by P. V. Kamat and D. Meisel (Elsevier, Amsterdam, 1997), pp. 353–461.
[8] J. M. Bennett, E. Pelletier, G. Albrand, J. P. Borgogno, B. Lazarides, C. K. Carniglia, R. A. Schmell, T. H. Allen, T. Tuttle-Hart, K. H. Guenther, and A. Saxer, Appl. Opt. **28**, 3303 (1989).
[9] G. Parjadis de Lariviere, J. M. Frigerio, J. Rivory, and F. Abeles, Appl. Opt. **31**, 6056 (1992).
[10] J. P. Borgogno, F. Flory, P. Roche, B. Schmitt, G. Albrand, E. Pelletier, and H. A. Macleod, Appl. Opt. **23**, 3567 (1984).
[11] M. M. Rahman, G. Yu, K. Murali Krishna, T. Soga, J. Watanabe, T. Jimbo, and M. Umeno, Appl. Opt. **37**, 691 (1998).
[12] M. M. Rahman, T. Miki, K. M. Krishna, T. Soga, K. Igarashi, S. Tanemura, and M. Umeno, Mater. Sci. Eng., B **41**, 67 (1996).
[13] M. Gartner, C. Parlog, and P. Osiceanu, Thin Solid Films **234**, 561 (1993).
[14] C. K. Carnigla, J. Opt. Soc. Am. A **7**, 848 (1990).
[15] D. E. Aspnes and J. B. Theeten, Phys. Rev. B **20**, 3292 (1979).
[16] T. Gerfin and M. Gratzel, J. Appl. Phys. **79**, 1722 (1996).
[17] JCPDS Powder Diffraction File Cards (1994) for TiO_2, 21-1272 (anatase), and 21-1272 (rutile).
[18] J. Yuan and S. Tsujikawa, J. Electrochem. Soc. **142**, 3444 (1995).
[19] B. D. Cullity, *Elements of X-ray Diffraction* (Addison–Wesley, Reading, MA, 1978), p. 99.
[20] K. Kato, A. Tsuge, and K. Nihara, J. Am. Ceram. Soc. **79**, 1483 (1996).
[21] S. Y. Kim, Appl. Opt. **35**, 6703 (1996).
[22] K. A. Vorotilov, E. V. Orlova, and V. I. Petrovsky, Thin Solid Films **207**, 180 (1992).
[23] P. G. Pai, S. S. Chao, Y. Takagi, and G. Lucovsky, J. Vac. Sci. Technol. A **4**, 689 (1986).
[24] Y. Mishima, M. Takei, T. Uematsu, N. Matsumoto, T. Kakehi, U. Wakino, and M. Okabe, J. Appl. Phys. **78**, 217 (1995).